# Lawrence Berkeley National Laboratory
## Recent Work


### Title
Four-Spin Terms and the Origin of the Chiral Spin Liquid in Mott Insulators on the Triangular Lattice.


### Permalink
https://escholarship.org/uc/item/5dn93158



### Journal
Physical review letters, 127(8)

### ISSN
0031-9007



### Authors
Cookmeyer, Tessa
Motruk, Johannes
Moore, Joel E



### Publication Date
2021-08-01

### DOI
10.1103/physrevlett.127.087201

Peer reviewed



eScholarship.org Powered by the California Digital Library
University of California

# Four-Spin Terms and the Origin of the Chiral Spin Liquid in Mott Insulators on the Triangular Lattice

Tessa Cookmeyer,[1,2*] Johannes Motruk,[1,2,3] and Joel E. Moore[1,2]

[1]Department of Physics, University of California, Berkeley, California 94720, USA

[2]Materials Sciences Division, Lawrence Berkeley National Laboratory, Berkeley, California 94720, USA

[3]Department of Theoretical Physics, University of Geneva, Quai Ernest-Ansermet 30, 1205 Geneva, Switzerland

At strong repulsion, the triangular-lattice Hubbard model is described by $s = 1/2$ spins with nearest-neighbor antiferromagnetic Heisenberg interactions and exhibits conventional 120° order. Using the infinite density matrix renormalization group and exact diagonalization, we study the effect of the additional four-spin interactions naturally generated from the underlying Mott-insulator physics of electrons as the repulsion decreases. Although these interactions have historically been connected with a gapless ground state with emergent spinon Fermi surface, we find that, at physically relevant parameters, they stabilize a chiral spin liquid (CSL) of Kalmeyer-Laughlin (KL) type, clarifying observations in recent studies of the Hubbard model. We then present a self-consistent solution based on a mean-field rewriting of the interaction to obtain a Hamiltonian with similarities to the parent Hamiltonian of the KL state, providing a physical understanding for the origin of the CSL.

*Introduction.*—The triangular lattice has played a prominent role in the physics of spin liquids ever since they were first proposed by Anderson [1], and many of the candidate materials exhibit this lattice geometry [2–11]. In particular, some organic charge transfer salts [2,3] and $1T$-$TaS_2$ [6,12] are believed to be described by the Hubbard model on the triangular lattice in the vicinity of the Mott transition. While the existence of a nonmagnetic insulating (NMI) phase in the Hubbard model has been observed in numerous studies [13–23], the determination of the type of spin-liquid phase in direct studies of the Hubbard model has long been elusive.

The problem has instead often been investigated via an effective spin model. Deep in the insulating phase of the Hubbard model, a nearest-neighbor Heisenberg model is sufficient and contains long-ranged three-sublattice order [24–26]. To describe physics closer to the Mott transition, one includes a four-spin ring-exchange part in addition to the Heisenberg term, a description coming from the lowest order $t/U$ expansion of the Hubbard model [27]. In a seminal paper, Motrunich showed, using variational Monte Carlo simulations, that a spin liquid with spinon Fermi surface (SFS) is a strong competitor for the ground state if the ring-exchange term is large enough [28]. Indications for this state, in subsequent works also referred to as spin-Bose metal, have been seen in other studies, including some with complementary methods [12,17,29–32], but remain under debate [33]. However, recent work on the Hubbard model suggested that the NMI is instead a chiral spin liquid (CSL) of Kalmeyer-Laughlin (KL) type [34–38], seemingly at odds with the results for the effective spin model.

In this Letter, using a combination of exact diagonalization (ED) and infinite density matrix renormalization group (iDMRG) [39] simulations, we first show that the KL spin liquid is indeed the ground state of the effective spin model around the parameter regime relevant for the Hubbard model. We demonstrate that this CSL does not emerge as a competing state to the SFS, but rather appears at a different value of the four-spin interaction; this is to our knowledge the first demonstration of a KL ground state in a time-reversal invariant spin model on the triangular lattice. However, we also find that much of the region that had been attributed to the SFS in previous works is occupied by a magnetically ordered zigzag state. The second main result is to connect analytically the four-spin term, which preserves time-reversal symmetry (TRS), back to the TRS-breaking parent Hamiltonians of the KL state [40,41] by mean-field arguments. Hence, one aspect of our work clarifies the relation between the appearance of the CSL in the triangular-lattice Hubbard model and the corresponding spin model, while the second clarifies why the CSL appears in the spin model via a connection to known TRS-breaking parent Hamiltonians for the CSL.

Finding a parent spin Hamiltonian of the KL state [40,41] and its generalizations, the Read-Rezayi states [42,43], has been of considerable interest. Generally, the parent Hamiltonians derived from conformal-field theoretic (CFT) arguments have long-ranged interactions, but a local Hamiltonian can be found if only short-ranged coefficients are kept, made uniform, and tuned [41,43–47]. While the underlying Hamiltonian for a material in zero applied field should respect TRS, these parent Hamiltonians explicitly break TRS. A notable exception is on the kagome lattice near a classical chiral phase transition [48–53], but no TRS-preserving spin Hamiltonian with KL ground state on the triangular lattice is known analytically.

*Model.*—Motivated by the $t/U$ expansion of the Hubbard model, we consider the following Hamiltonian:

$$H = J_1 \sum_{\langle ij \rangle} \boldsymbol{S}_i \cdot \boldsymbol{S}_j + J_2 \sum_{\langle\langle ij \rangle\rangle} \boldsymbol{S}_i \cdot \boldsymbol{S}_j + H_4, \quad (1)$$

where $\langle ij \rangle$ ($\langle\langle ij \rangle\rangle$) denotes (next-)nearest neighbor pairs. The four-spin interaction $H_4$ is given by

$$H_4 = J_4 \sum_{\langle i,j,k,l \rangle} [(\boldsymbol{S}_i \cdot \boldsymbol{S}_j)(\boldsymbol{S}_k \cdot \boldsymbol{S}_l) + (\boldsymbol{S}_i \cdot \boldsymbol{S}_l)(\boldsymbol{S}_j \cdot \boldsymbol{S}_k) - (\boldsymbol{S}_i \cdot \boldsymbol{S}_k)(\boldsymbol{S}_j \cdot \boldsymbol{S}_l)], \quad (2)$$

where $\langle i,j,k,l \rangle$ denotes a sum over unique rhombuses as defined by unique next-nearest neighbor pairs $\langle\langle ik \rangle\rangle$ (see Fig. 1). This four-spin term is related to the extensively studied ring-exchange operator [12,28–31,33,54–62] via the $4J_2 = J_4$ line. Furthermore, studies on the $J_4 = 0$ line have focused on the emergence of a "$J_1$-$J_2$ spin liquid" [45,46,63–68]. Treated classically, the Hamiltonian exhibits spontaneous TRS breaking into a tetrahedrally ordered phase [69–73], further motivating this particular model. From here on in, we take $J_1 = 1$ and $\sum_i S_i^z = 0$.

*Exact diagonalization.*—We perform ED on $6 \times 4$ spins with periodic boundary conditions (PBCs). The PBCs are chosen such that the unit cell is translated in the $\hat{y}$ direction and in the $2\hat{x} - \hat{y}$ direction. We compute the structure factor for the spin $\boldsymbol{S}_i$ and dimer $D_\alpha^{\boldsymbol{x}_i} = \boldsymbol{S}_{\boldsymbol{x}_i} \cdot \boldsymbol{S}_{\boldsymbol{x}_i+\boldsymbol{\alpha}}$ correlations

$$S(\boldsymbol{q}) = \sum_{i,j} (\langle \boldsymbol{S}_i \cdot \boldsymbol{S}_j \rangle - \langle \boldsymbol{S}_i \rangle \cdot \langle \boldsymbol{S}_j \rangle) e^{i\boldsymbol{q}\cdot(\boldsymbol{x}_j - \boldsymbol{x}_i)}, \quad (3)$$

$$D_\alpha(\boldsymbol{q}) = \sum_{i,j} (\langle D_\alpha^{\boldsymbol{x}_i} D_\alpha^{\boldsymbol{x}_j} \rangle - \langle D_\alpha^{\boldsymbol{x}_i} \rangle \langle D_\alpha^{\boldsymbol{x}_j} \rangle) e^{i\boldsymbol{q}\cdot(\boldsymbol{x}_j - \boldsymbol{x}_i)}, \quad (4)$$

with $\boldsymbol{\alpha}$ being the vector to one of the three nearest neighbors, and $\boldsymbol{S}_{\boldsymbol{x}_i}$ is an alternative notation for $\boldsymbol{S}_i$. Large values of $S(\boldsymbol{q})$ and/or $D_\alpha(\boldsymbol{q})$ indicate ordered phase; see [73] for more information about the various orders.

To distinguish the tetrahedral from the collinear state, we compute a nematic order parameter, a chiral-chiral order parameter, [46] and we study the effect of adding a small TRS-breaking term to the Hamiltonian. As shown in the Supplemental Material [73], this analysis clearly shows that large $S(M')$ [$S(M)$] is indicative of tetrahedral (collinear) order.

Additionally, we are most interested in checking whether the chiral spin-liquid phase appears. For that reason, we compute $\mathcal{O}_{\mathrm{CFT}} = \sqrt{\sum_{i=1}^{4} |\langle \psi | \mathrm{KL}_i \rangle|^2}$, the overlap of the ground state with its projection into the subspace spanned

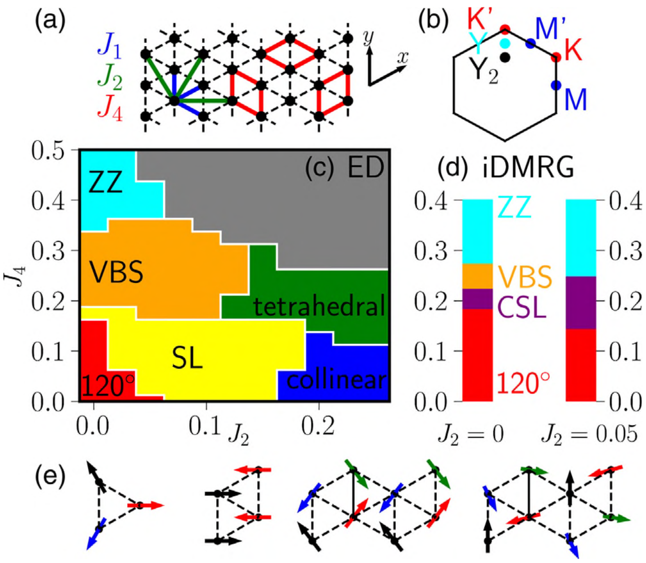


FIG. 1. (a) The different colored lines connect the spins involved in the different terms of Eq. (1). (b) The first Brillouin zone of the lattice showing several named points. (c) The proposed phase diagram from our ED results using the various orders in Fig. 2. For phase descriptions, see the Supplemental Material [73]. The phase boundaries were determined via the symmetry sector of the ground state and first excited state [46,73]. The grayed out region is within the SFS parameter space found in [28], but also might have some dimer or plaquette ordering. (d) The phase diagram from the iDMRG results on the $L_y = 6$ cylinder on the $J_2 = 0.00$, 0.05 slices, which includes the CSL, perhaps suggested by ED. (e) From left to right, the 120°, collinear, zigzag (ZZ), and tetrahedral (whose spins, connected tail to tail, form a tetrahedron) classical spin orders are shown [73].

by the four orthonormalized KL states $|\mathrm{KL}_i\rangle$ (given explicitly in Ref. [85]). The degeneracy comes from a combination of twofold topological and TRS-breaking degeneracy each.

From all of the data presented in Fig. 2, we see that there are potentially many ordered states, and we present a phase diagram in Fig. 1(c). Most interesting, however, is that, in the region most relevant for the Hubbard model at small $J_2$ and $J_4 \sim 0.1$–$0.15$, the overlap with the CSL is large.

*iDMRG.*—In order to investigate this tendency on larger system sizes, we focus on the region with $J_2 \leq 0.05$ and $J_4 \leq 0.4$ and study it with iDMRG. We consider the model on infinite cylinders of circumferences $L_y = 6$ and 8 sites and compute the ground state on the slices $J_2 = 0$ and $J_2 = 0.05$ at various bond dimensions $\chi_{\mathrm{BD}}$. We use the TeNPy library [86] and give further details of the numerics in the Supplemental Material [73]. The results for the $L_y = 6$ cylinder are presented in Fig. 3 and are summarized in Fig. 1(d). We find similar phases as in ED. The spins order into the 120° (zigzag) state at low (high) $J_4$, respectively. At intermediate $J_4$, we find a phase that breaks TRS by acquiring a nonzero value of the chiral order parameter $\chi = \langle \boldsymbol{S}_i \cdot (\boldsymbol{S}_j \times \boldsymbol{S}_k) \rangle$ with $i$, $j$, $k$ going clockwise around a

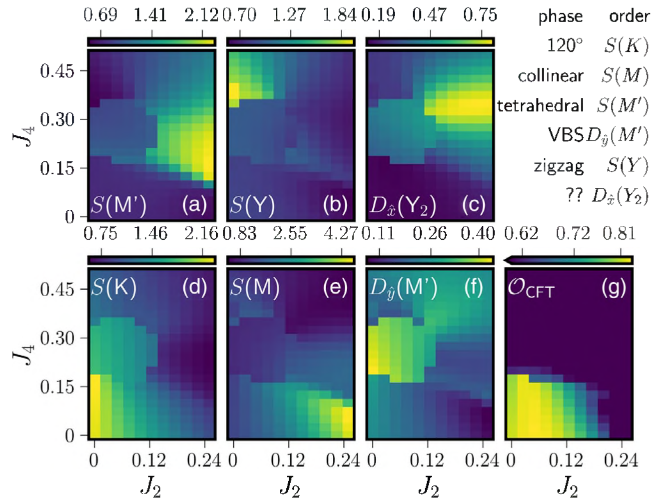


FIG. 2. (a)–(f) Various orders are shown in color vs $J_2$ and $J_4$. The table in the upper right indicates the phase to which each order corresponds. (g) The overlap of the ground state with the manifold of KL states, which suggests that the CSL may appear for small $J_2$ and $J_4$.

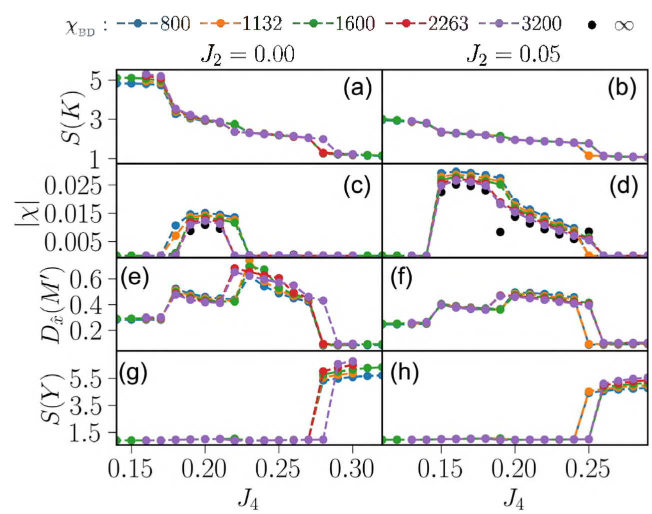


FIG. 3. We plot various order parameters that we extract from ground state wave function from iDMRG for the $L_y = 6$ cylinder, and $J_2 = 0$ ($J_2 = 0.05$) for the left (right) column, respectively. (a),(b) [(g),(h)] We plot the spin-spin correlation at the $K$ ($Y$) point, respectively. We see a jump in the value corresponds to a phase boundary. (c),(d) We plot $\chi = \langle \boldsymbol{S}_i \cdot (\boldsymbol{S}_j \times \boldsymbol{S}_k) \rangle$ averaged over all triangles of the lattice from the iDMRG results at varying bond dimension $\chi_{\mathrm{BD}}$. (d) The jump in the nonzero value of $\chi$ at $J_4 = 0.19$ corresponds to whether the trivial ($J_4 \le 0.19$) or semion ($J_4 \ge 0.20$) sector of the KL state is the ground state as evidenced by the entanglement spectra. We include an extrapolation [73] to $\chi_{\mathrm{BD}} \to \infty$ where it is nonzero. (e),(f) We plot the dimer-dimer correlation at the $M'$ point for dimers in the $\hat{x}$ direction, which signals the VBS state. The phase boundaries estimated from these data are plotted in Fig. 1.

triangle (and $\langle \cdot \rangle$ denotes the expectation averaged over all triangles in the lattice), which we identify as the KL CSL below. Furthermore, we confirm the presence of the valence-bond solid (VBS) on the $J_2 = 0$ slice reported in Ref. [12].

For the $L_y = 8$ cylinder, we focus on demonstrating that, at the point $(J_2, J_4) = (0.05, 0.18)$, the ground state is the CSL. By running the algorithm at different $(J_2, J_4)$, we find the same states as in the $L_y = 6$ cylinder. In addition to an unbiased run, we use those states as the initial state to bias the algorithm toward converging to a non-CSL state at (0.05,0.18). By $\chi_{\mathrm{BD}} = 1600$, however, the algorithm always converges to the CSL, and an unbiased run with $\chi_{\mathrm{BD}} = 3200$ also finds the CSL.

*Identification as the CSL.*—Here, we identify the TRS-breaking phase as the Kalmeyer-Laughlin state by studying the entanglement spectrum and performing a spin-Hall numerical experiment. We focus on $(J_2, J_4) = (0.05, 0.18)$ and show the results of both in Fig. 4. First, we compute the entanglement spectrum, which shows the correct counting for the KL state; each of the levels with spin quantum number $|s_z| \in \{0, 1, 2\}$ show the degeneracy pattern of $1, 1, 2, 3, 5, \ldots$ as we move around the momentum [87,88].

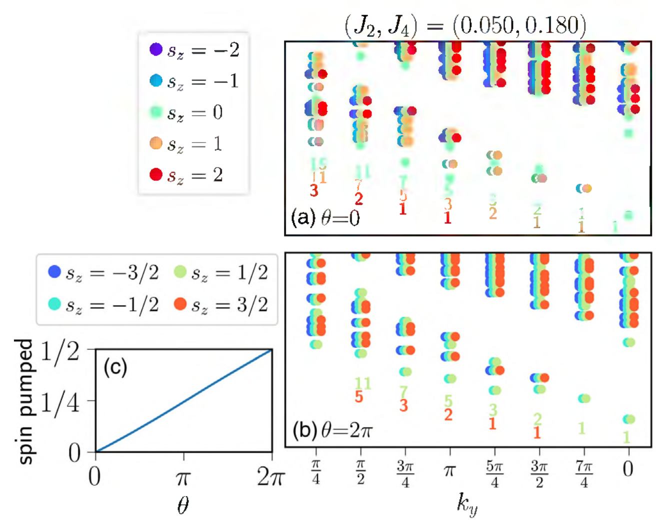


FIG. 4. (a) We plot the entanglement spectrum for the ground state at $(J_2, J_4) = (0.05, 0.18)$ on the $L_y = 8$ cylinder with $\chi_{\mathrm{BD}} = 1600$. The $y$ axis is $-s \ln(s)$, where $s$ are the Schmidt values. The color indicates the charge as specified in the legend, and different charges are offset slightly from each other to more clearly show the degeneracy. For each momentum, the counting of the lowest cluster of Schmidt values is shown for each of the $s_z \ge 0$ charges in color. They show the correct pattern for the Kalmeyer-Laughlin state. (b) We make the same plot as in (a) after adiabatically inserting one flux quantum through the cylinder. Although the Hamiltonian is the same, the entanglement spectrum has changed, indicating a topological degeneracy of the state. (c) During the flux insertion, we can monitor how much spin has flowed along the cylinder. We see that exactly a spin $1/2$ is pumped across the system, indicating a quantized fractional spin-Hall effect.

Next, we thread flux through the cylinder by replacing $S_i^+ S_j^- \to S_i^+ S_j^- e^{i\theta(y_i - y_j)/L_y}$, so that, upon going around the cylinder, a spin will have picked up a phase of $e^{i\theta}$. As can be seen in Fig. 4(c), adding $2\pi$ flux moves exactly $1/2$ a spin along the cylinder. Additionally, although the Hamiltonian has returned to the original Hamiltonian up to a gauge transformation, the ground state has a different entanglement spectrum with half-integer spin quantum numbers. Indeed, inserting $2\pi$ flux exchanges the trivial and semion sectors of the ground state manifold [89] of the KL state on the infinite cylinder, which is precisely what we see in this numerical experiment.

*Zigzag vs spinon Fermi surface.*—In a recent DMRG study of Eq. (1) at $J_2 = 0$, the authors of Ref. [12] find a spin liquid at $J_4 \gtrsim 0.3$ that they identify as a spinon Fermi surface phase. We instead find that a zigzag ordered state at finite bond dimension has lower energy for the parameter choices we studied (i.e., $J_4 \leq 0.4$), consistent with our ED results. By biasing the initial state toward the SFS or zigzag state, we compare how the energy depends on the truncation error of iDMRG at the point $J_4 = 0.4$ [73,90,91], which allows us to estimate the ground state energy at infinite bond dimension. However, we still find the zigzag state is preferred for the $L_y = 6$ cylinder where we performed the analysis. Future work may attempt to clarify whether the SFS appears at other points in the parameter space; a recent effort in that direction is seen in [33]. Regardless, the SFS does not seem to be favored in the regime most physically close to the Hubbard model. These results could also be investigated by variational Monte Carlo studies, since previous works seem not to have considered a trial state with zigzag order [28,31,59].

*Discussion.*—As mentioned in the Introduction, this spin model is motivated by the Hubbard model's $t/U$ expansion. In particular, at order $t^4/U^3$, the Hubbard model gives $J_1 = 4(1 - 7t^2/U^2)t^2/U$, $J_2 = 4t^4/U^3$, $J_3 = 4t^4/U^3$, and $J_4 = 80t^4/U^3$, where $J_3$ is a next-next-nearest-neighbor Heisenberg interaction [27]. Ignoring $J_3$, if we use the value of $U/t \sim 10.6$ for the transition to the CSL phase from Ref. [35], we would estimate the transition to be at $(J_2, J_4) \sim (0.01, 0.19)$, essentially where we find it.

One could still ask why the KL state should be the ground state for the Hamiltonian (1), though. In this section, we connect the above Hamiltonian to the parent Hamiltonians of Refs. [41–43]. In the Supplemental Material [73], we derive that, for spin 1/2s, we can rewrite Eq. (2) as

$$H_4 = -\frac{107}{88} J_4 \sum_{\langle ij \rangle} \boldsymbol{S}_i \cdot \boldsymbol{S}_j + 3NJ_4 \frac{129}{352} + J_4 \sum_{\langle i,j,k,l \rangle} \left( -\frac{39}{88} \hat{\chi}_{ijkl}^2 - \frac{21}{22} (\hat{\chi}_{ijkl}^2)^2 + \frac{8}{11} (\hat{\chi}_{ijkl}^2)^3 \right), \quad (5)$$

where $\hat{\chi}_{ijkl}^2 = \mathcal{O}_\triangle(i,j,l)\mathcal{O}_\triangledown(k,l,j) + O_\triangledown(k,l,j) \cdot \mathcal{O}_\triangle(i,j,l)$ for $\mathcal{O}_{\triangle/\triangledown}(i,j,k) = 2\boldsymbol{S}_i \cdot (\boldsymbol{S}_j \times \boldsymbol{S}_k)$, and $N$ is the number of sites.

We now mean-field decouple $(\hat{\chi}_{ijkl}^2)^n$. In the phase we are looking for, the scalar chirality $\chi = \langle O_\triangle(i,j,k) \rangle / 2 = \langle O_\triangledown(i,j,k) \rangle / 2$ takes a nonzero value on all triangles. Rewriting $\mathcal{O}_{\triangle/\triangledown}/2 = \chi + \epsilon_{\triangle/\triangledown}$, expanding, and keeping only to order $\epsilon$, we arrive at the Hamiltonian

$$H = \left( J_1 - \frac{107}{88} J_4 \right) \sum_{\langle ij \rangle} \boldsymbol{S}_i \cdot \boldsymbol{S}_j + J_2 \sum_{\langle\langle ij \rangle\rangle} \boldsymbol{S}_i \cdot \boldsymbol{S}_j + 3NJ_4 \frac{129}{352} + 3NJ_4 \left( \frac{39}{11}\chi^2 + \frac{63}{22} 8^2 \chi^4 - \frac{5}{11} 8^4 \chi^6 \right) + \underbrace{3J_4 \left[ -\frac{39}{11}\chi - \frac{21}{11} 8^2 \chi^3 + \frac{3}{11} 8^4 \chi^5 \right]}_{J_\chi} \sum_{\triangle,\triangledown} \boldsymbol{S}_i \cdot (\boldsymbol{S}_j \times \boldsymbol{S}_k). \quad (6)$$

By adjusting $J_4$ and $J_2$, we are essentially following the program of localizing the long-range parent Hamiltonian of Refs. [40–43]; however, we also have self-consistency conditions. In semiquantitative agreement with the iDMRG results [Fig. 1(d)], we show that when $J_2/[J_1 - (107/88)J_4] = 0.05$ the point $J_4 = 0.13$ produces a self-consistent solution with $\chi \approx -0.116$ and $J_\chi/[J_1 - (107/88)J_4] \approx 0.268$ [73], whose ground state is known to be the KL state [45,46]. We note that the mean-field decoupling happens only on the level of the chiral order parameter and the ground state of the resulting Hamiltonian (6) still has to be found by iDMRG.

Further evidence in support of the validity of this rewriting comes from the similarity of the phase diagram of Eq. (1) at intermediate $J_4$ in comparison to the phase diagram of the $J_1$-$J_2$-$J_\chi$ Hamiltonian at intermediate $J_\chi$ studied in Refs. [45,46]. In particular, we find the three most relevant competing phases for $J_4 = 0.16$ are the 120° order, the CSL, and the tetrahedral order [73], in analogy to $J_\chi \sim 0.2$. Additionally, the rewriting in Eq. (5) is reminiscent of the analysis in Ref. [92] where the nearest-neighbor term is rewritten as related to $[\boldsymbol{S}_i \cdot (\boldsymbol{S}_j \times \boldsymbol{S}_k)]^2$. The author then writes down and analyzes a free-energy expression to argue that TRS is spontaneously broken when $J_2 \neq 0$. Although that is not seen in numerics, future work could apply a similar analysis to our Eq. (5).

*Conclusion.*—We have demonstrated that a CSL appears in the effective spin model for the Hubbard model on the triangular lattice at half filling in the parameter space near the physically relevant region. Furthermore, through a rewriting of Eq. (1), we heuristically argued that the CSL emerges in this model because the four-spin term favors spontaneous TRS breaking, after which the mean-field Hamiltonian resembles known parent Hamiltonians of the KL state. This result provides some understanding of the origin of the CSL in the Hubbard model found in Refs. [35,38]. We additionally have found that the SFS may only be the ground state in a more restricted part of the phase diagram than previously thought. Beyond the triangular lattice, the approach of seeking self-consistent numerical solutions of a mean-field-decoupled Hamiltonian could potentially aid in understanding the appearance of spin liquids in some other situations.

We thank Aaron Szasz and Mike Zaletel for helpful conversations and collaboration on related work. This work was supported as part of the Center for Novel Pathways to Quantum Coherence in Materials, an Energy Frontier Research Center funded by the U.S. Department of Energy, Office of Science, Basic Energy Sciences. T. C. was supported by NSF DGE 1752814 and NSF DMR-1918065. J. M. received funding through DFG research Fellowship No. MO 3278/1-1 and TIMES at Lawrence Berkeley National Laboratory, supported by the U.S. Department of Energy, Office of Basic Energy Sciences, Division of Materials Sciences and Engineering, under Award No. DE-AC02-76SF00515. J. E. M. acknowledges support from a Simons Investigatorship. Numerical computations were performed on the Lawrencium cluster at Lawrence Berkeley National Laboratory.

*Note added.*—A recent preprint [93], using a heuristic Schwinger boson argument, may provide an alternative understanding of the origin of the KL state in this model.

*tcookmeyer@berkeley.edu

[1] P. Anderson, Resonating valence bonds: A new kind of insulator?, Mater. Res. Bull. **8**, 153 (1973).

[2] Y. Shimizu, K. Miyagawa, K. Kanoda, M. Maesato, and G. Saito, Spin Liquid State in an Organic Mott Insulator with a Triangular Lattice, Phys. Rev. Lett. **91**, 107001 (2003).

[3] T. Itou, A. Oyamada, S. Maegawa, M. Tamura, and R. Kato, Quantum spin liquid in the spin-1/2 triangular antiferromagnet $\mathrm{EtMe_3Sb[Pd(dmit)_2]_2}$, Phys. Rev. B **77**, 104413 (2008).

[4] Y. Li, H. Liao, Z. Zhang, S. Li, F. Jin, L. Ling, L. Zhang, Y. Zou, L. Pi, Z. Yang, J. Wang, Z. Wu, and Q. Zhang, Gapless quantum spin liquid ground state in the two-dimensional spin-1/2 triangular antiferromagnet $\mathrm{YbMgGaO_4}$, Sci. Rep. **5**, 16419 (2015).

[5] Y. Shen *et al.*, Evidence for a spinon Fermi surface in a triangular-lattice quantum-spin-liquid candidate, Nature (London) **540**, 559 (2016).

[6] K. T. Law and P. A. Lee, 1T-$\mathrm{TaS_2}$ as a quantum spin liquid, Proc. Natl. Acad. Sci. U.S.A. **114**, 6996 (2017).

[7] A. Ribak, I. Silber, C. Baines, K. Chashka, Z. Salman, Y. Dagan, and A. Kanigel, Gapless excitations in the ground state of $1T-\mathrm{TaS_2}$, Phys. Rev. B **96**, 195131 (2017).

[8] M. Klanjšek, A. Zorko, R. Žitko, J. Mravlje, Z. Jagličić, P. K. Biswas, P. Prelovšek, D. Mihailovic, and D. Arčon, A high-temperature quantum spin liquid with polaron spins, Nat. Phys. **13**, 1130 (2017).

[9] K. Y. Zeng, L. Ma, Y. X. Gao, Z. M. Tian, L. S. Ling, and L. Pi, NMR study of the spin excitations in the frustrated antiferromagnet $\mathrm{Yb(BaBO_3)_3}$ with a triangular lattice, Phys. Rev. B **102**, 045149 (2020).

[10] N. Li, Q. Huang, X. Y. Yue, W. J. Chu, Q. Chen, E. S. Choi, X. Zhao, H. D. Zhou, and X. F. Sun, Possible itinerant excitations and quantum spin state transitions in the effective spin-1/2 triangular-lattice antiferromagnet $\mathrm{Na_2BaCo(PO_4)_2}$, Nat. Commun. **11**, 4216 (2020).

[11] R. Sarkar, P. Schlender, V. Grinenko, E. Haeussler, P. J. Baker, T. Doert, and H.-H. Klauss, Quantum spin liquid ground state in the disorder free triangular lattice $\mathrm{NaYbS_2}$, Phys. Rev. B **100**, 241116(R) (2019).

[12] W.-Y. He, X. Y. Xu, G. Chen, K. T. Law, and P. A. Lee, Spinon Fermi Surface in a Cluster Mott Insulator Model on a Triangular Lattice and Possible Application to $1T-\mathrm{TaS_2}$, Phys. Rev. Lett. **121**, 046401 (2018).

[13] H. Morita, S. Watanabe, and M. Imada, Nonmagnetic insulating states near the Mott transitions on lattices with geometrical frustration and implications for $\kappa$-$\mathrm{(ET)_2Cu_2(CN)_3}$, J. Phys. Soc. Jpn. **71**, 2109 (2002).

[14] B. Kyung and A. M. S. Tremblay, Mott Transition, Antiferromagnetism, and *d*-Wave Superconductivity in Two-Dimensional Organic Conductors, Phys. Rev. Lett. **97**, 046402 (2006).

[15] P. Sahebsara and D. Sénéchal, Hubbard Model on the Triangular Lattice: Spiral Order and Spin Liquid, Phys. Rev. Lett. **100**, 136402 (2008).

[16] R. T. Clay, H. Li, and S. Mazumdar, Absence of Superconductivity in the Half-Filled Band Hubbard Model on the Anisotropic Triangular Lattice, Phys. Rev. Lett. **101**, 166403 (2008).

[17] H.-Y. Yang, A. M. Läuchli, F. Mila, and K. P. Schmidt, Effective Spin Model for the Spin-Liquid Phase of the Hubbard Model on the Triangular Lattice, Phys. Rev. Lett. **105**, 267204 (2010).

[18] T. Yoshioka, A. Koga, and N. Kawakami, Quantum Phase Transitions in the Hubbard Model on a Triangular Lattice, Phys. Rev. Lett. **103**, 036401 (2009).

[19] L. F. Tocchio, A. Parola, C. Gros, and F. Becca, Spin-liquid and magnetic phases in the anisotropic triangular lattice: The case of $\kappa-\mathrm{(ET)_2X}$, Phys. Rev. B **80**, 064419 (2009).

[20] A. E. Antipov, A. N. Rubtsov, M. I. Katsnelson, and A. I. Lichtenstein, Electron energy spectrum of the spin-liquid state in a frustrated Hubbard model, Phys. Rev. B **83**, 115126 (2011).

[21] M. Laubach, R. Thomale, C. Platt, W. Hanke, and G. Li, Phase diagram of the Hubbard model on the anisotropic triangular lattice, Phys. Rev. B **91**, 245125 (2015).

[22] T. Shirakawa, T. Tohyama, J. Kokalj, S. Sota, and S. Yunoki, Ground-state phase diagram of the triangular lattice Hubbard model by the density-matrix renormalization group method, Phys. Rev. B **96**, 205130 (2017).

[23] K. Misumi, T. Kaneko, and Y. Ohta, Mott transition and magnetism of the triangular-lattice Hubbard model with next-nearest-neighbor hopping, Phys. Rev. B **95**, 075124 (2017).

[24] D. A. Huse and V. Elser, Simple Variational Wave Functions for Two-Dimensional Heisenberg Spin-1/2 Antiferromagnets, Phys. Rev. Lett. **60**, 2531 (1988).

[25] B. Bernu, P. Lecheminant, C. Lhuillier, and L. Pierre, Exact spectra, spin susceptibilities, and order parameter of the

quantum Heisenberg antiferromagnet on the triangular lattice, Phys. Rev. B **50**, 10048 (1994).

[26] L. Capriotti, A. E. Trumper, and S. Sorella, Long-Range Néel Order in the Triangular Heisenberg Model, Phys. Rev. Lett. **82**, 3899 (1999).

[27] A. H. MacDonald, S. M. Girvin, and D. Yoshioka, $t/U$ expansion for the Hubbard model, Phys. Rev. B **37**, 9753 (1988).

[28] O. I. Motrunich, Variational study of triangular lattice spin-$1/2$ model with ring exchanges and spin liquid state in $\kappa-(\mathrm{ET})_2\mathrm{Cu}_2(\mathrm{CN})_3$, Phys. Rev. B **72**, 045105 (2005).

[29] D. N. Sheng, O. I. Motrunich, and M. P. A. Fisher, Spin Bose-metal phase in a spin-$\frac{1}{2}$ model with ring exchange on a two-leg triangular strip, Phys. Rev. B **79**, 205112 (2009).

[30] M. S. Block, D. N. Sheng, O. I. Motrunich, and M. P. A. Fisher, Spin Bose-Metal and Valence Bond Solid Phases in a Spin-$1/2$ Model with Ring Exchanges on a Four-Leg Triangular Ladder, Phys. Rev. Lett. **106**, 157202 (2011).

[31] R. V. Mishmash, J. R. Garrison, S. Bieri, and C. Xu, Theory of a Competitive Spin Liquid State for Weak Mott Insulators on the Triangular Lattice, Phys. Rev. Lett. **111**, 157203 (2013).

[32] Q.-R. Zhao and Z.-X. Liu, Thermal properties and instability of a $U(1)$ spin liquid on the triangular lattice, arXiv:2105.08413.

[33] A. M. Aghaei, B. Bauer, K. Shtengel, and R. V. Mishmash, Efficient matrix-product-state preparation of highly entangled trial states: Weak Mott insulators on the triangular lattice revisited, arXiv:2009.12435.

[34] V. Kalmeyer and R. B. Laughlin, Equivalence of the Resonating-Valence-Bond and Fractional Quantum Hall States, Phys. Rev. Lett. **59**, 2095 (1987).

[35] A. Szasz, J. Motruk, M. P. Zaletel, and J. E. Moore, Chiral Spin Liquid Phase of the Triangular Lattice Hubbard Model: A Density Matrix Renormalization Group Study, Phys. Rev. X **10**, 021042 (2020).

[36] Z. Zhu, D. N. Sheng, and A. Vishwanath, Doped Mott insulators in the triangular lattice Hubbard model, arXiv:2007.11963.

[37] A. Szasz and J. Motruk, Phase diagram of the anisotropic triangular lattice Hubbard model, Phys. Rev. B **103**, 235132 (2021).

[38] B.-B. Chen, Z. Chen, S.-S. Gong, D. N. Sheng, W. Li, and A. Weichselbaum, Quantum spin liquid with emergent chiral order in the triangular-lattice Hubbard model, arXiv:2102.05560.

[39] I. P. McCulloch, Infinite size density matrix renormalization group, revisited, arXiv:0804.2509.

[40] R. Thomale, E. Kapit, D. F. Schroeter, and M. Greiter, Parent Hamiltonian for the chiral spin liquid, Phys. Rev. B **80**, 104406 (2009).

[41] A. E. B. Nielsen, G. Sierra, and J. I. Cirac, Local models of fractional quantum Hall states in lattices and physical implementation, Nat. Commun. **4**, 2864 (2013).

[42] M. Greiter, D. F. Schroeter, and R. Thomale, Parent Hamiltonian for the non-Abelian chiral spin liquid, Phys. Rev. B **89**, 165125 (2014).

[43] I. Glasser, J. I. Cirac, G. Sierra, and A. E. B. Nielsen, Exact parent Hamiltonians of bosonic and fermionic Moore-Read states on lattices and local models, New J. Phys. **17**, 082001 (2015).

[44] B. Bauer, L. Cincio, B. P. Keller, M. Dolfi, G. Vidal, S. Trebst, and A. W. W. Ludwig, Chiral spin liquid and emergent anyons in a kagome lattice Mott insulator, Nat. Commun. **5**, 5137 (2014).

[45] S.-S. Gong, W. Zhu, J.-X. Zhu, D. N. Sheng, and K. Yang, Global phase diagram and quantum spin liquids in a spin-$\frac{1}{2}$ triangular antiferromagnet, Phys. Rev. B **96**, 075116 (2017).

[46] A. Wietek and A. M. Läuchli, Chiral spin liquid and quantum criticality in extended $s=\frac{1}{2}$ Heisenberg models on the triangular lattice, Phys. Rev. B **95**, 035141 (2017).

[47] C. Hickey, L. Cincio, Z. Papić, and A. Paramekanti, Emergence of chiral spin liquids via quantum melting of noncoplanar magnetic orders, Phys. Rev. B **96**, 115115 (2017).

[48] L. Messio, B. Bernu, and C. Lhuillier, Kagome Antiferromagnet: A Chiral Topological Spin Liquid?, Phys. Rev. Lett. **108**, 207204 (2012).

[49] S.-S. Gong, W. Zhu, and D. Sheng, Emergent chiral spin liquid: Fractional quantum Hall effect in a kagome Heisenberg model, Sci. Rep. **4**, 6317 (2014).

[50] Y.-C. He, D. N. Sheng, and Y. Chen, Chiral Spin Liquid in a Frustrated Anisotropic Kagome Heisenberg Model, Phys. Rev. Lett. **112**, 137202 (2014).

[51] A. Wietek, A. Sterdyniak, and A. M. Läuchli, Nature of chiral spin liquids on the kagome lattice, Phys. Rev. B **92**, 125122 (2015).

[52] W.-J. Hu, W. Zhu, Y. Zhang, S. Gong, F. Becca, and D. N. Sheng, Variational Monte Carlo study of a chiral spin liquid in the extended Heisenberg model on the kagome lattice, Phys. Rev. B **91**, 041124(R) (2015).

[53] S.-S. Gong, W. Zhu, L. Balents, and D. N. Sheng, Global phase diagram of competing ordered and quantum spin-liquid phases on the kagome lattice, Phys. Rev. B **91**, 075112 (2015).

[54] G. Misguich, B. Bernu, and C. Lhuillier, The multiple-spin exchange phase diagram on the triangular lattice: Schwinger-boson analysis, J. Low Temp. Phys. **110**, 327 (1998).

[55] K. Kubo, H. Sakamoto, T. Momoi, and K. Niki, A possible magnetic phase with scalar chirality in solid 3He layers, J. Low Temp. Phys. **111**, 583 (1998).

[56] G. Misguich, C. Lhuillier, B. Bernu, and C. Waldtmann, Spin-liquid phase of the multiple-spin exchange Hamiltonian on the triangular lattice, Phys. Rev. B **60**, 1064 (1999).

[57] W. LiMing, G. Misguich, P. Sindzingre, and C. Lhuillier, From Néel long-range order to spin liquids in the multiple-spin exchange model, Phys. Rev. B **62**, 6372 (2000).

[58] Y. Fuseya and M. Ogata, Phase diagram of the triangular $t-J$ model with multiple spin exchange in the doped-Mott region, J. Phys. Soc. Jpn. **78**, 013601 (2009).

[59] T. Grover, N. Trivedi, T. Senthil, and P. A. Lee, Weak Mott insulators on the triangular lattice: Possibility of a gapless nematic quantum spin liquid, Phys. Rev. B **81**, 245121 (2010).

[60] M. Holt, B. J. Powell, and J. Merino, Spin-liquid phase due to competing classical orders in the semiclassical theory of the Heisenberg model with ring exchange on an anisotropic triangular lattice, Phys. Rev. B **89**, 174415 (2014).

[61] K. Riedl, R. Valentí, and S. M. Winter, Critical spin liquid versus valence-bond glass in a triangular-lattice organic antiferromagnet, Nat. Commun. **10**, 2561 (2019).
[62] K. Seki and S. Yunoki, Thermodynamic properties of an $S = \frac{1}{2}$ ring-exchange model on the triangular lattice, Phys. Rev. B **101**, 235115 (2020).
[63] R. Kaneko, S. Morita, and M. Imada, Gapless spin-liquid phase in an extended spin $1/2$ triangular Heisenberg model, J. Phys. Soc. Jpn. **83**, 093707 (2014).
[64] Z. Zhu and S. R. White, Spin liquid phase of the $S = \frac{1}{2}$ $J_1 - J_2$ Heisenberg model on the triangular lattice, Phys. Rev. B **92**, 041105(R) (2015).
[65] W.-J. Hu, S.-S. Gong, W. Zhu, and D. N. Sheng, Competing spin-liquid states in the spin-$\frac{1}{2}$ Heisenberg model on the triangular lattice, Phys. Rev. B **92**, 140403(R) (2015).
[66] S. N. Saadatmand and I. P. McCulloch, Detection and characterization of symmetry-broken long-range orders in the spin-$\frac{1}{2}$ triangular Heisenberg model, Phys. Rev. B **96**, 075117 (2017).
[67] S.-S. Gong, W. Zheng, M. Lee, Y.-M. Lu, and D. N. Sheng, Chiral spin liquid with spinon Fermi surfaces in the spin-$\frac{1}{2}$ triangular Heisenberg model, Phys. Rev. B **100**, 241111(R) (2019).
[68] S. Hu, W. Zhu, S. Eggert, and Y.-C. He, Dirac Spin Liquid on the Spin-1/2 Triangular Heisenberg Antiferromagnet, Phys. Rev. Lett. **123**, 207203 (2019).
[69] S. E. Korshunov, Chiral phase of the Heisenberg antiferromagnet with a triangular lattice, Phys. Rev. B **47**, 6165 (1993).
[70] K. Kubo and T. Momoi, Ground state of a spin system with two- and four-spin exchange interactions on the triangular lattice, Z. Phys. B **103**, 485 (1997).
[71] T. Momoi, K. Kubo, and K. Niki, Possible Chiral Phase Transition in Two-Dimensional Solid $^3$He, Phys. Rev. Lett. **79**, 2081 (1997).
[72] L. Messio, C. Lhuillier, and G. Misguich, Lattice symmetries and regular magnetic orders in classical frustrated antiferromagnets, Phys. Rev. B **83**, 184401 (2011).
[73] See Supplemental Material at http://link.aps.org/supplemental/10.1103/PhysRevLett.127.087201 for information on the connection to the Hubbard model, the classical phase diagram, description of the methods, additional numerical data and a detailed derivation of the mean-field argument, which includes Refs. [74–84].
[74] F. Wang and A. Vishwanath, Spin-liquid states on the triangular and kagomé lattices: A projective-symmetry-group analysis of Schwinger boson states, Phys. Rev. B **74**, 174423 (2006).
[75] F. Pollmann, S. Mukerjee, A. M. Turner, and J. E. Moore, Theory of Finite-Entanglement Scaling at One-Dimensional Quantum Critical Points, Phys. Rev. Lett. **102**, 255701 (2009).
[76] H. Fehske, R. Schneider, and A. Weiße, *Computational Many-Particle Physics* (Springer, New York, 2007), Vol. 739, https://link.springer.com/book/10.1007%2F978-3-540-74686-7.
[77] A. Wietek, M. Schuler, and A. M. Läuchli, Studying continuous symmetry breaking using energy level spectroscopy, arXiv:1704.08622.
[78] S. R. White, Density matrix renormalization group algorithms with a single center site, Phys. Rev. B **72**, 180403(R) (2005).
[79] G. M. Crosswhite and D. Bacon, Finite automata for caching in matrix product algorithms, Phys. Rev. A **78**, 012356 (2008).
[80] J. Motruk, M. P. Zaletel, R. S. K. Mong, and F. Pollmann, Density matrix renormalization group on a cylinder in mixed real and momentum space, Phys. Rev. B **93**, 155139 (2016).
[81] L. Cincio and G. Vidal, Characterizing Topological Order by Studying the Ground States on an Infinite Cylinder, Phys. Rev. Lett. **110**, 067208 (2013).
[82] H.-H. Tu, Y. Zhang, and X.-L. Qi, Momentum polarization: An entanglement measure of topological spin and chiral central charge, Phys. Rev. B **88**, 195412 (2013).
[83] M. P. Zaletel, R. S. K. Mong, and F. Pollmann, Topological Characterization of Fractional Quantum Hall Ground States from Microscopic Hamiltonians, Phys. Rev. Lett. **110**, 236801 (2013).
[84] M. P. Zaletel, R. S. K. Mong, F. Pollmann, and E. H. Rezayi, Infinite density matrix renormalization group for multicomponent quantum Hall systems, Phys. Rev. B **91**, 045115 (2015).
[85] A. E. B. Nielsen and G. Sierra, Bosonic fractional quantum Hall states on the torus from conformal field theory, J. Stat. Mech. (2014) P04007.
[86] J. Hauschild and F. Pollmann, Efficient numerical simulations with tensor networks: Tensor Network Python (TeNPy), SciPost Phys. Lect. Notes, 5 (2018).
[87] X. G. Wen, Gapless boundary excitations in the quantum Hall states and in the chiral spin states, Phys. Rev. B **43**, 11025 (1991).
[88] H. Li and F. D. M. Haldane, Entanglement Spectrum as a Generalization of Entanglement Entropy: Identification of Topological Order in Non-Abelian Fractional Quantum Hall Effect States, Phys. Rev. Lett. **101**, 010504 (2008).
[89] Though degenerate in the thermodynamic limit, the energy of the semion and trivial sector differ by 0.04% (0.1%) on the $L_y = 8$ ($L_y = 6$) cylinder, respectively, at $(J_2, J_4) = (0.05, 0.18)$.
[90] O. Legeza and G. Fáth, Accuracy of the density-matrix renormalization-group method, Phys. Rev. B **53**, 14349 (1996).
[91] C. Hubig, J. Haegeman, and U. Schollwöck, Error estimates for extrapolations with matrix-product states, Phys. Rev. B **97**, 045125 (2018).
[92] G. Baskaran, Novel Local Symmetries and Chiral-Symmetry-Broken Phases in $S = (1/2)$ Triangular-Lattice Heisenberg Model, Phys. Rev. Lett. **63**, 2524 (1989).
[93] Q. Zhang and T. Li, On the origin of the possible chiral spin liquid state of the triangular lattice Hubbard model, arXiv:2103.10714.